Variation and Calibration Error in Electronic Imaging

Peter D. Burns
Eastman Kodak Company
Rochester, NY USA

Abstract

In acquiring digital images, electronic systems not only detect optical signals but also convert them into a digital form for further image processing and exchange. Practical systems can introduce error during color calibration, and when acquiring image scene information. For large populations it is often assumed that the error can be modeled as a random variable having a zero mean. In the case of a single color instrument, camera or scanner, however, error due to deterioration of a physical standard, optical filter or detector will introduce a bias into the measurement or image data. This error is modified as the signals are transformed (processed) into their final form. An error-propagation method is shown to describe the influence of the data-processing path on the magnitude of bias error. This approach is related to the propagation of image noise, or variance. The analysis is applied in examples drawn from color-measurement and digital image processing.

Introduction

When making color measurements, we can think of instrument uncertainty as introducing an error into the (color) signal of interest. The same can be said of the acquisition of a digital image where pixel-to-pixel noise and color calibration errors can occur. We often assume that the error can be modeled as a random variable having a zero mean. For a single color instrument, however, a calibration error can introduce a consistent bias.

Color-measurement signals and digital images are usually transformed between several common color spaces. Therefore, an analysis of the way signal transformations influence the magnitude of color-signal error is useful when comparing performance with system tolerances.[1,2] These results can then be used to set limits for both instruments and physical standards.

One tool for the evaluation of error or variation in signal processing is error-propagation analysis,[3] where specific signal processing steps can be described by their corresponding transformations of the error statistics. The most common use of this method is the propagation of the second-order statistics, variance and RMS error.

Livens[4] addressed the combination of stochastic instrument errors and signal quantization. He showed that the combined variance is found by adding the effective variance of each noise source, as for independent sources. Gonzalez, *et al.*, evaluated the practical limits to color accuracy in terms of the color-difference metric, ΔE^*_{94}. They compared results with and without color management, and pointed out requirements for ICC device profiles.

In this paper, we address the propagation of first-order statistical error, bias. This can be applied to a consistent error component due to, e.g., instrument drift, deterioration of a physical standard, or signal quantization.

Bias Error

If an observed signal is subject to error, it can be expressed as the sum of true value and bias,

$$\hat{p} = p + b_p ,$$

where $\hat{p}$ is the observed value, p the true value, and b_p the bias error. For many measurements or digital images, both the true and bias values vary, so we can define the bias using statistical expectations

$$b_p = \mathrm{E}[\hat{p}] - \mu_p \ , \qquad (1)$$

where E is the expected value and μ_p is the true (unbiased) mean.

A matrix-vector notation is usually adopted for systems with related sets of (color) signals. This is used in the Appendix, where the transformation, or scaling, of the bias error due to signal transformations is approximated using a derivative matrix in Eq. (a7).

Matrix

The propagation of bias error for a simple matrix transformation of a set of color signals can be understood as a special case of Eq. (a6). For example,

$$\mathbf{q} = \mathbf{M}\mathbf{p} \ . \qquad (2)$$

Since each element of the matrix, **M**, is a constant, the elements of the first derivative matrix, $\mathbf{J_M}$, are simply the matrix coefficients. The resulting bias in **q** is,

$$\mathbf{b_q} \cong \mathbf{M}\mathbf{b_p}. \qquad (3)$$

XYZ to CIELAB

Bias error propagation for a common colorimetric transformation, from tristimulus values (*X,Y,Z*) to CIELAB coordinates (*L*, a*, b**) can be also be modeled. Here we assume that the bias in the measured tristimulus values is that evident after the division by those of the white reference, (X_n, Y_n, Z_n). For values of X/X_n, Y/Y_n, $Z/Z_n > 0.00886$ the derivative matrix is

$$\mathbf{J} = \begin{bmatrix} 0 & \frac{116}{3\mu_Y^{2/3}} & 0 \\ \frac{500}{3\mu_X^{2/3}} & -\frac{500}{3\mu_Y^{2/3}} & 0 \\ 0 & \frac{200}{3\mu_Y^{2/3}} & -\frac{200}{3\mu_Z^{2/3}} \end{bmatrix}. \qquad (4)$$

The bias propagation is given by Eq. (a6),

$$\mathbf{b_{L^*a^*b^*}} \cong \mathbf{J}\ \mathbf{b_{XYZ}}. \qquad (5)$$

McDowell[6] gave several 'rules of thumb' for the propagation of reflectance factor measurement error to CIELAB. He investigated the relationship between spectral reflectance error and CIELAB ΔE^*_{ab} using the 928 color patches of the ANSI IT8.7/3 CMYK output characterization target.

He found that a neutral 2% change in the measured *X*, *Y*, *Z* values (from reflectance factor measurements) resulted in an average ΔE^*_{ab} of 0.5 and a maximum of 0.9. If, however, the error was in the *Z* value, due to yellowing of the white reference, the average ΔE^*_{ab} was 0.9. Similarly, leaving the *Y* and *Z* values unchanged and changing the *X* value by 2% resulted in an average $\Delta E^*_{ab} = 1.8$.

If we interpret these instrument errors as bias introduced into the *X, Y, Z* values, the above error-propagation analysis can be compared with McDowell's computed results. This was done and the results do predict the actual measurement results. Table 1 summarizes the comparison. Figure 1 shows the ΔE^*_{ab} that results from a 2% nonselective bias, plotted as an *a*-b** surface for *L** = 50.

Table 1: Comparison of bias analysis, via Eq. (4) and McDowell results (*in italic*), for the IT8 data set.

	% bias			ΔE^*_{ab}	
	X	Y	Z	average	max.
Nonselective	-2	-2	-2	0.46 *0.5*	0.87 *0.9*
Low X	-2	0	0	1.80 *1.8*	3.01 *3.0*
Low Y	0	-2	0	1.96	3.32
Yellowing	0	0	-2	0.68 *0.7*	1.18 *1.2*

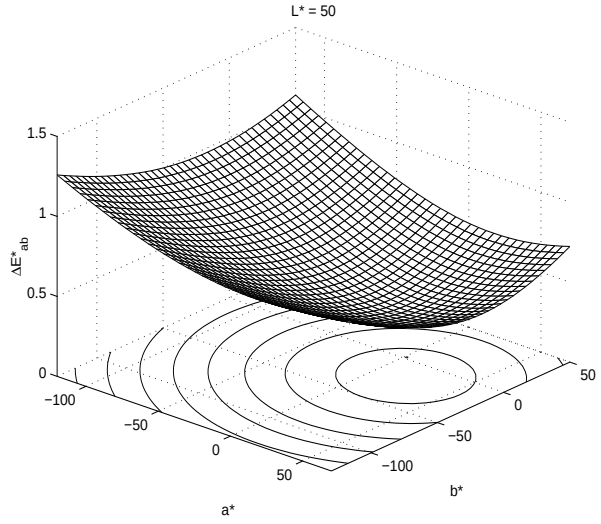

Figure 1. ΔE^*_{ab} *for 2% bias in* X, Y, Z *for* L* = *50*

CRT Gamma

A common color encoding specification for the interchange of digital images is sRGB.[7,8] This was developed to facilitate viewing of images on computer CRTs, and so includes the color characteristics of a reference monitor. This reference monitor is characterized by the monitor phosphor tristimulus values, and (mean) signal transfer function. The transfer function is modeled by an equation for output luminance.[9] For an input signal, *d*, [0-1] the resulting CRT luminance factor is

$$I = (k_1 d + k_2)^{\gamma}, \qquad (6)$$

where k_1 and k_2 are the system gain and offset and γ is the CRT gamma. In general, the gain and offset values are under the control of the user, by way of the contrast and brightness controls. The gamma value is primarily set by the CRT design. Since most CRT color evaluations require estimation of the effective gamma, it is useful to understand the

sensitivity of the above luminance model to variations in the gamma value. If a monitor deviates from expected performance by a bias in the gamma value, the bias propagation is given by Eq. (a4)

$$b_I = \left(d^{\mu_\gamma} \log_e d\right) b_\gamma \quad , \qquad (7)$$

where k_1 and k_2 have been set to 1 and 0. For a true value of $\mu_\gamma = 2.2$ and bias, $b_\gamma = 0.15$, Fig. 2 shows the CRT transfer curves. The luminance factor bias that would result from this gamma error was then computed directly and via Eq. (7), with the results plotted in Fig. 3. The overestimation of the negative bias is due to the series approximation of Eqs. (a4) and (a6).

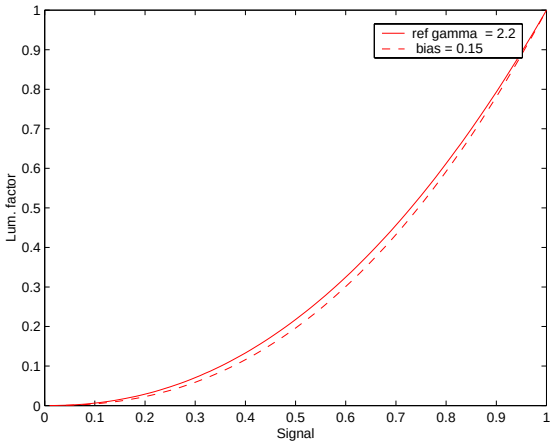

Figure 2. CRT characteristics: μ_γ = 2.2 and b_γ = 0.15

The derivative matrix of Eq. (4) was then used to propagate the luminance factor error to CIELAB. The resulting bias in L^* is plotted in Fig. 4. We again observe good agreement between bias error-propagation and direct calculation.

Conclusions

The analysis of the propagation of bias errors during signal processing can be used in conjunction with direct error computation. In all cases described, the error propagation method gave similar results to those computed directly. The method, therefore, can be expected to provide predictions of color measurement and calibration performance for a wide range of practical transformations. In many cases, the error transformations can be inverted, facilitating their application to component tolerancing and subsystem specification.

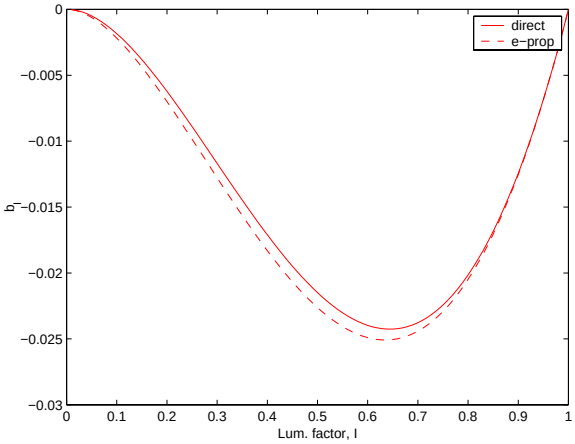

Figure 3. Luminance factor [0-1] bias for b_γ = 0.15. The solid line is the point-by-point difference, dashed is from bias equation.

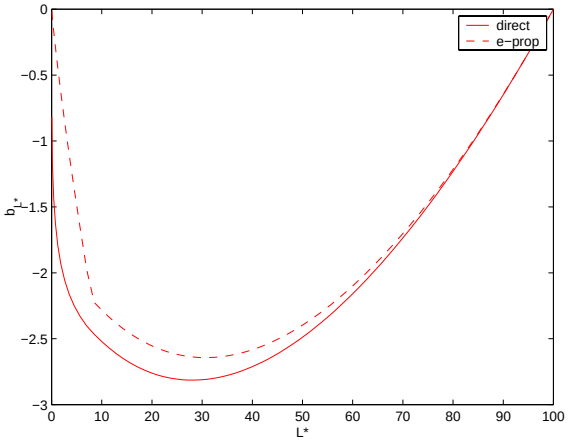

Figure 4. Bias in L due to b_γ =0.15, (in L* units [0-100]).Solid line is the point-by-point difference, dashed is from bias equations.*

Acknowledgements
Many thanks to David McDowell for sharing his experience and data, and Gustav Braun for his suggestions.

References

1. M. Stokes, M. D. Fairchild and R. S. Bern, *ACM Trans. on Graphics*, 11, pg. 406, (1992).
2. J. E. Gibson, M. D. Fairchild and S. L. Wright, 'Colorimetric Tolerances of Various Digital Image Displays', *Proc. IS&T/SID Eighth Color Imaging Conference*, pg. 296, (2000).
3. P. D. Burns and R. S. Berns, *Color Research and Appl.*, 22, 280 (1997).
4. S. Livens, 'The Effect of Quantisation Error on the Accuracy of Colour Transforms, *Proc. IS&T/SID Eighth Color Imaging Conference*, pg. 70, (2000).

5. G. Gonzalez, T. Hecht, A. Ritzer, A. Paul, J.-F. Le Nest and M. Has, 'Color Management-How accurate need it be?', *Proc. IS&T/SID Fifth Color Imaging Conference*, pg. 270, (1997).
6. D. Q. McDowell, 'The Relationship Between Uncertainty in Reflectance Factor Data and Computed CIELAB values, Some Intuitive Tools,' *Proc. SPIE*, 3648, pg. 291, (1998).
7. M. Stokes, M. Anderson, S. Chandrasekar and R. Motta, 'A Standard Default Color Space for the Internet: sRGB', available at http://www.w3.org/Graphics/Color/sRGB.html, 1996.
8. 'Multimedia systems and equipment - Colour measurement and management – Part2-1: Colour management – Default RGB colour space – sRGB', Standard 61966-2-1, IEC, http://www.iec.ch, 1999.
9. E. J. Giorgianni and T. E. Madden, Digital Color Management: encoding solutions, Addison Wiley, Reading Mass., pg. 60-65, 1998.

Appendix: Bias of a Function of a Biased Random Variable

We are given the function $f(x)$ of the random variable, x, which is corrupted with a bias error. If $\hat{x}$ is the biased random variable, its expected value can be written as

$$E[\hat{x}] = b_x + \mu_x, \quad (a1)$$

where b_x is the bias and μ_x is the true (expected) value. We define the bias of $f(x)$ as

$$b_f = \mathrm{E}[f(\hat{x})] - f(\mu_x) \qquad (a2)$$

If we expand f about μ_x in a Taylor series and take expectations

$$E[f(\hat{x})] \cong f(\mu_x) + f'(\mu_x) b_x + 0.5 f''(\mu_x)\sigma_x^2, \quad (a3)$$

where

$$f'(\mu_x) = \left.\frac{\partial f}{\partial x}\right|_{x=\mu_x} \text{ and } f''(\mu_x) = \left.\frac{\partial^2 f}{\partial^2 x}\right|_{x=\mu_x}.$$

Substituting Eq. (a3) into Eq. (a2), the bias error in $f(x)$ can be approximated by

$$b_f \cong f' b_x + 0.5 f'' \sigma_x^2.$$

The RHS shows the two components of the bias in f. The first is due to the bias in $\hat{x}$ and the second due to its variation. Here we will only consider the first source, bias, since it will usually dominate, so

$$b_f \cong f' b_x. \qquad (a4)$$

Similar expressions can be developed for multivariate transformations. Let **x** and **y** be vectors, related by **f**

$$\mathbf{y} = \mathbf{f}(\mathbf{x}), \qquad (a5)$$

where

$$\mathbf{x} = [x_1, x_2, ..., x_n]^{\mathrm{T}}, \ \mathbf{y} = [y_1, y_2, ..., y_m]^{\mathrm{T}},$$

$$\mathbf{f}(\mathbf{x}) = \begin{bmatrix} f_1(x_1, x_2, \cdots, x_n) \\ f_2(x_1, x_2, \cdots, x_n) \\ \vdots \\ f_m(x_1, x_2, \cdots, x_n) \end{bmatrix}.$$

For color image processing, m and n are often equal to 3. If the bias in each component signal of **x** is written as a vector

$$\mathbf{b_x} = [b_{x_1}, b_{x_2}, \cdots, b_{x_n}]^{\mathrm{T}},$$

the output bias vector is

$$\mathbf{b_y} \cong \mathbf{J_f} \mathbf{b_x}, \qquad (a6)$$

where

$$\mathbf{J_f} = \begin{bmatrix} \frac{\partial y_1}{\partial x_1} & \frac{\partial y_1}{\partial x_2} & \cdots & \frac{\partial y_1}{\partial x_n} \\ \frac{\partial y_2}{\partial x_1} & \ddots & & \\ \vdots & & \ddots & \\ \frac{\partial y_m}{\partial x_1} & & & \frac{\partial y_m}{\partial x_n} \end{bmatrix}. \qquad (a7)$$

Each element of $\mathbf{J_f}$ is evaluated at $(\mu_{x_1}, \mu_{x_2}, \cdots, \mu_{x_n})$.

Biography

Peter Burns studied Electrical and Computer Engineering at Clarkson University, receiving his B.Sc. and M.Sc. degrees. In 1997, he completed his Ph.D. in Imaging Science at Rochester Institute of Technology. After working for Xerox, he joined Eastman Kodak Company, where he works in Electronic Imaging Products, Research and Development. A frequent contributor to imaging conferences, his technical interests include; system evaluation, simulation, and the statistical analysis of error in digital and hybrid systems. peter.burns@kodak.com